Controller-Hardware-in-the-Loop Testing of A Single-Phase Single-Stage Transformerless Grid-Connected Photovoltaic Inverter

Mohammadi, Fazel and Bok, Rasoul and Hajian, Masood and Rezaei-Zare, Afshin

28 February 2022

Controller-Hardware-in-the-Loop Testing of A Single-Phase Single-Stage Transformerless Grid-Connected Photovoltaic Inverter

Fazel Mohammadi, *Senior Member, IEEE,* Rasoul Bok, Masood Hajian, *Senior Member, IEEE*, and Afshin Rezaei-Zare, *Senior Member, IEEE*

***Abstract*—In this paper, the validation and performance testing of a control scheme for a single-phase single-stage transformerless grid-connected Photovoltaic (PV) inverter are presented using the Control-Hardware-in-the-Loop (C-HIL) implementation. The control scheme uses the DC–link voltage controller and grid current controller, and it is executed in a LAUNCHXL-F28379D development kit, providing a cost-effective solution compared to commercially available tools. In order to extract the maximum available power from the PV system under different conditions, two Maximum Power Point Tracking (MPPT) algorithms, including the Perturb and Observe (P&O) algorithm and incremental conductance method, are investigated and compared. The simulation and experimental results are provided to verify the performance of the studied control scheme.**

***Index Terms*—Controller-Hardware-in-the-Loop (C-HIL), Digital Control, Grid-Connected Inverter, Maximum Power Point Tracking (MPPT) Algorithm, Photovoltaic (PV) Systems.**

I. Introduction

NOWADAYS, the need for renewable energy has greatly increased. Among Renewable Energy Sources (RESs), Photovoltaic (PV) systems are of great interest due to their availability, emission-free operating principle, and lower cost of maintenance [1][2]. Based on policies and regulatory support by power utilities, PV systems deployment can be done for power grids resilience enhancement. In order for PV systems to inject power into power grids, specific standards and grid-connection performance requirements should be considered to ensure safety and power quality [3].

The PV inverter is one of the main components of PV systems, which converts the DC power from the PV array into AC power. However, the harmonics level is a controversial issue for the majority of PV inverters. Based on IEEE Standard 1547–2018 and IEC 61727:2004, the current Total Harmonic Distortion (THD) should be limited to 5% [4][5]. In addition, harmonic components should be restricted to 4% for odd harmonics from 3rd to 9th order and 2% for 11th to 15th order. Such inverters can also use Maximum Power Point Tracking (MPPT) algorithms to extract the maximum amount of energy from the PV array [6]. Different MPPT algorithms, such as the Perturb and Observe (P&O) algorithm and incremental conductance method, and their operating principles are reviewed in [7]. Indeed, the reference signal for the DC–link voltage can be generated by the MPPT algorithm. The operating principle of the P&O algorithm is based on the continuous perturbation of the DC–link voltage till the maximum power point can be achieved [8]. In addition, the incremental conductance method uses the instantaneous conductance and the incremental conductance for tracking the maximum power point [9].

There are different types of PV inverters topologies for central, string, multi-string, and micro architectures, including cascaded H-bridge inverters, diode clamped inverters, etc. [10][11]. Single-phase H-bridge inverters are commonly used in PV systems due to their simplicity in design and implementation [12][13]. To control PV inverters, different approaches, such as current controller with the grid voltage feed-forward [14], current controller with feed-forward DC-voltage regulator [15], second-order generalized integrator [16], resonant control with harmonics compensator [17], synchronous voltage control [18], are investigated.

This paper aims at proposing a control scheme for a single-phase single-stage transformerless grid-connected PV inverter. The presented control scheme consists of the DC–link voltage controller, current controller, and grid synchronization based on Phase Locked Loop (PLL). In order to extract the maximum power from the PV array, the P&O algorithm and incremental conductance method are investigated and compared. In addition, to assess the performance of the presented control scheme, the Control-Hardware-in-the-Loop (C-HIL) testing using a LAUNCHXL-F28379D development kit is performed. The obtained simulation and experimental results show the applicability and effectiveness of the presented control scheme.

The rest of this paper is organized as follows. The control strategy is described in Section II. Results and discussions are provided in Section III. Finally, Section IV concludes this paper.

II. Control Strategy

A. Power Flow Equations

Figure 1 shows the system configuration of a single-phase single-stage transformerless grid-connected PV system. Neglecting the inverter, the DC–link capacitor, and the output filter losses, the instantaneous power balance in the DC–link can be formulated as follows:

$$P_{pv}(t) = P_C(t) + P_g(t) \tag{1}$$

Fazel Mohammadi (corresponding author) and Afshin Rezaei-Zare are with the Department of Electrical Engineering and Computer Science, York University, Toronto, ON, M3J 1P3, Canada (e-mail: fazel@yorku.ca, fazel.mohammadi@ieee.org; rezaei@yorku.ca).

Rasoul Bok and Masood Hajian are with the Department of Electrical and Computer Engineering, Isfahan University of Technology, Isfahan 84156-83111, Iran (e-mail: rasool.bok@ec.iut.ac.ir; m.hajian@iut.ac.ir).

978-1-6654-7902-8/22/$31.00 ©2022 IEEE

2022 IEEE Texas Power and Energy Conference (TPEC) | 978-1-6654-7902-8/22/$31.00 ©2022 IEEE | DOI: 10.1109/TPEC54980.2022.9750851

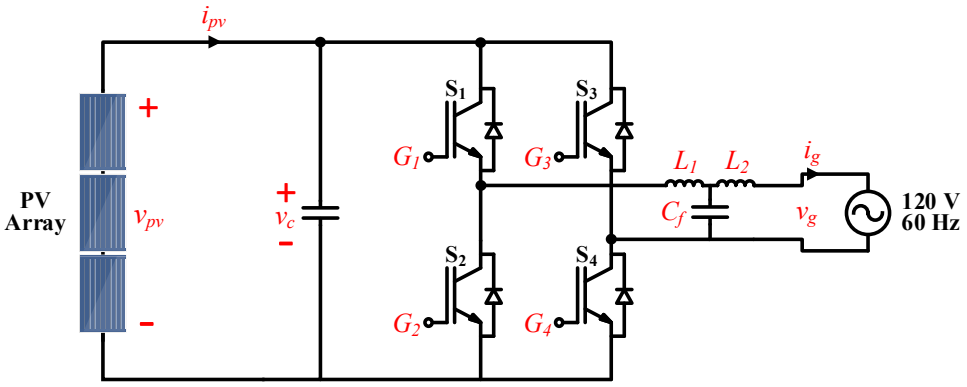

Figure 1. The system configuration of a single-phase single-stage transformerless grid-connected PV system.

where P_{pv}, P_C, and P_g are the instantaneous PV array power, instantaneous charge/discharge power of the DC–link capacitor, and instantaneous power fed into the power grid, respectively.

In addition,

$$\begin{cases} P_g(t) = v_g i_g = V_g I_g \left(1 - \cos(2\omega t)\right) \\ P_C(t) = CV_C \dfrac{dV_C}{dt} \end{cases} \tag{2}$$

where v_g and i_g denote the instantaneous voltage and current of the power grid, respectively, and V_g and I_g are the Root Mean Square (RMS) values of the power grid voltage and current, respectively. Furthermore, C and V_C show the size and the voltage across the DC–link capacitor, respectively.

B. Control Scheme

As shown in Figure 2, the presented control scheme consists of two main control loops. The external control loop is required to maintain a constant DC–link voltage and to ensure the correct function of the MPPT algorithm. The MPPT algorithm generates the reference voltage signal (v^*_{pv}). Since there is no component connected in series with the PV array, the PV array voltage and the DC–link voltage are equal. The DC–link voltage is then compared with the reference voltage signal while a Proportional–Integral (PI) controller minimizes the error between the reference voltage signal and the actual DC–link voltage. Due to the fact that the MPPT algorithm is rather slow, to improve the dynamics of the PV system in case of sudden changes in the PV array power, the gain $k_1 = \frac{\sqrt{2}}{V_g}$ is considered and added to the output of the DC–link voltage controller, resulting in the reference current signal (I^*_{ref}). The internal control loop is designed to control the power injected into the power grid. In order to impose a sinusoidal current (synchronized with the power grid voltage), the reference current signal I_{ref} is generated from a sinusoidal reference while its amplitude is regulated from the output of the external control loop. A Proportional–Resonant (PR) controller is then employed to minimize the error between the reference current signal and the actual output current. The structure of the implemented single-phase PLL is provided in Figure 3, which enables a unity power factor operation by synchronizing the output current of the inverter with the power grid voltage, generating a sinusoidal current reference signal, and also, monitoring the power grid voltage amplitude and frequency. The output of the current controller is then divided by the DC–link voltage to prevent over-modulation and the obtained signal is compared with a 10 kHz carrier signal to generate the Pulse Width Modulation (PWM) signals.

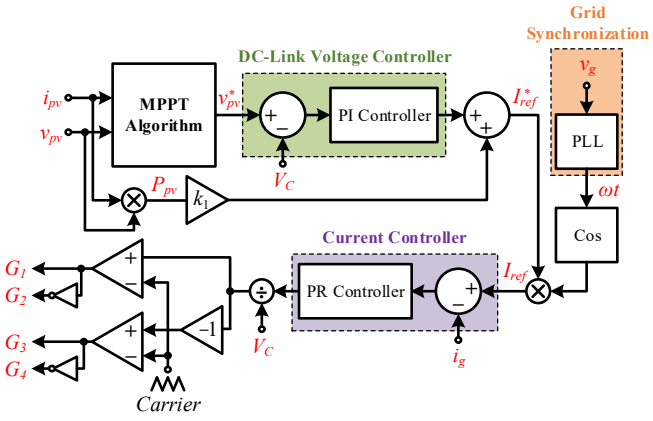

Figure 2. The presented control scheme for a single-stage single-phase transformerless grid-connected PV inverter.

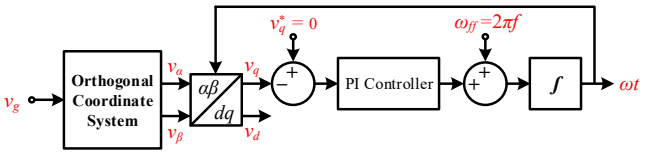

Figure 3. The structure of a single-phase PLL.

C. MPPT Algorithms

1) P&O Algorithm

Considering the characteristics of the PV module, in the P&O algorithm, the power variation (dP_{pv}) with respect to the voltage variation (dv_{pv}) at the maximum power point should be equal to zero while perturbations tend to direct the operating point in the maximum power point direction. In this regard, when $dP_{pv}>0$ and the operating voltage is perturbed in the direction of the maximum power point, the P&O algorithm continuously directs the voltage in the same direction. On the other side, if $dP_{pv}<0$, the P&O algorithm directs the perturbation in the opposite direction [7]. This

process leads to an increase/decrease in the DC voltage level and determines the reference voltage of the PV module under different conditions.

2) Incremental Conductance Method

The incremental conductance method can be considered as a specific implementation of the P&O algorithm. For a PV module, the incremental conductance method substitutes dP_{pv} with respect to dv_{pv} with the instantaneous current variation (di_{pv}) with respect to the voltage variation, resulting in the incremental conductance, i.e., $\frac{di_{pv}}{dv_{pv}}$, and finding the reference voltage of the PV module [7].

III. Results and Discussions

Figure 4 illustrates the C-HIL platform to validate the performance of the presented control scheme, which is executed by a LAUNCHXL-F28379D development kit. In the C-HIL platform, the actual controller is in the loop and the model of the entire single-phase single-stage transformerless grid-connected PV system is converted into executable codes. The generated codes are then transferred into the actual controller. The presented control scheme is implemented using a discrete time step of 1 μs, and the data is exchanged between the actual controller and the host computer using a Universal Serial Bus (USB) port. The C-HIL platform provides high-fidelity results for validation and verification purposes with approximately no commissioning cost and less safety risk.

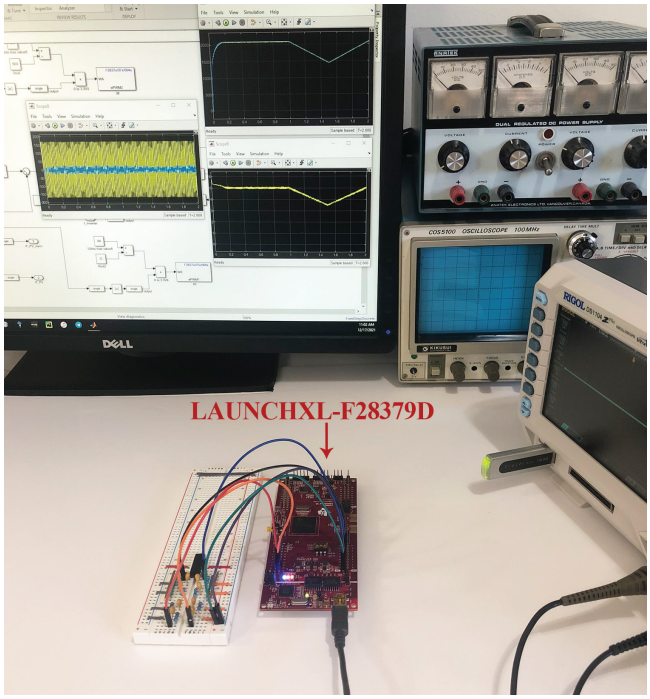

Figure 4. The experimental C-HIL platform.

The analyzed PV system consists of 11 series-connected modules in one parallel string with a nominal power of 190.16 W per module. The open–circuit voltage, short-circuit current, and voltage at the maximum power point of the PV system are 493.5 V, 5.5 A, and 415 V, respectively. A 1200 μF capacitor with no initial voltage is used as the DC–link capacitor and the switching frequency is 10 kHz. The LCL-filter consists of two 5 mH inductors and one 11 μF capacitor. The power grid nominal voltage and frequency are 120 V (RMS) and 60 Hz, respectively.

The simulation and experimental results for P&O algorithm and incremental conductance method under different scenarios are shown in Figures 5 and 6, where the initial solar irradiance and solar cell temperature are set to 1000 W/m^2 and 25 °C, respectively. The solar irradiance remains constant between t = 0 s and t = 1 s. Then, it decreases by 300 W/m^2 and reaches 700 W/m^2 at t = 1.5 s, and subsequently increases by 300 W/m^2 within 0.5 s and reaches its initial value at t = 2 s.

The PI controller $G_{\mathrm{PI}}(s)$ is defined as follows:

$$G_{\mathrm{PI}}(s) = 0.075 + \frac{0.075}{s} \tag{3}$$

In addition, the PR controller $G_{\mathrm{PR}}(s)$ is defined as follows:

$$G_{\mathrm{PR}}(s) = 10 + 400\frac{s}{s^2 + (2\pi f)^2} \tag{4}$$

where f is the power grid frequency.

A. P&O Algorithm

As shown in Figures 5(a) and 5(b), the P&O algorithm starts at t = 0.15 s, which is the time when the DC–link capacitor is fully charged and its voltage is equal to the open–circuit voltage of the PV array. The maximum voltage and current of the PV array using the P&O algorithm are 421.65 V and 5.10 A, respectively. According to the defined scenarios, by changing the solar irradiance between t = 1 s and t = 2 s, the voltage and current of the PV array deviate within the range of 406 V and 420 V and 3.5 A and 5.09 A, respectively. When atmospheric conditions are constant or vary with less dynamics, the P&O algorithm oscillates close to the maximum power point. The C-HIL experiment results show that the maximum voltage and current of the PV array using the P&O algorithm are 420.49 V and 5.09 A, respectively. This verifies the performance of the P&O algorithm.

As illustrated in Figures 5(c) and 5(d), when solar irradiance decreases, the PV array current proportionally decreases, which causes a reduction in injected current into the power grid. The voltage controller regulates the power grid voltage at 169.70 V. The maximum power grid current using the P&O algorithm is 25.3 A. However, variations in solar irradiance between t = 1 s and t = 2 s lead to changes in the power grid current within the range of 16.8 A and 25 A. In addition, the C-HIL experiment results show that the power grid current changes within the range of 16.14 A and 24.67 A.

As shown in Figure 5(e), the average PV array power and average power grid active power using the P&O algorithm are 1908.41 W and 1854.22 W, respectively. The minimum PV array power and power grid active power occur at t = 1.5 s, where the PV array power is 1455.31 W and the power grid active power is 1385.01 W. According to Figure 5(e), between t = 0.4 s and t = 0.6 s, the C-HIL experiment results show that the average PV array power and average power grid active power using the P&O algorithm are 1899.77 W and 1853.59 W, respectively. Therefore, the C-HIL experiment results confirm the applicability of the presented control scheme in real-world applications.

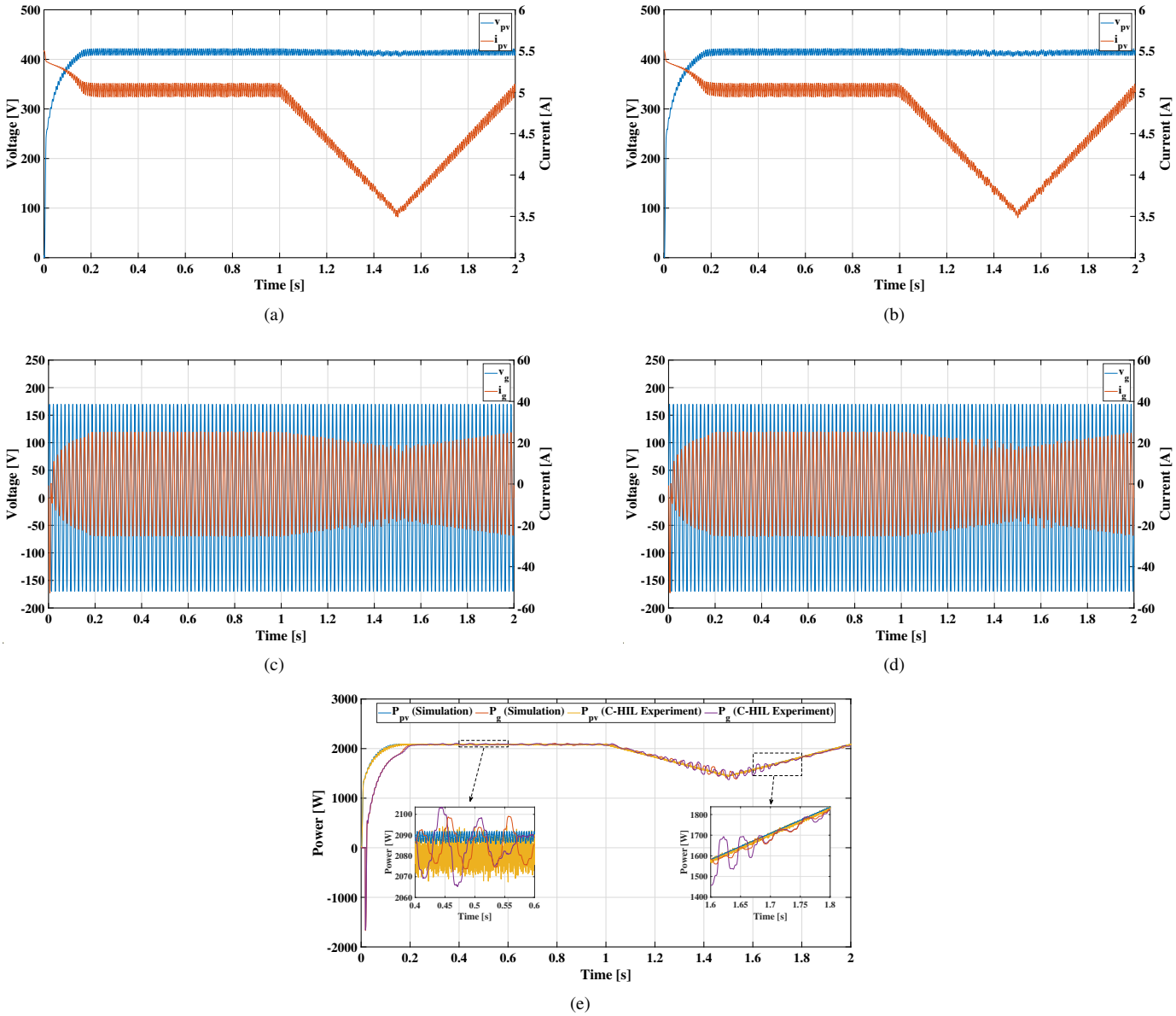

Figure 5. Results for the P&O algorithm, (a) PV array voltage and current (simulation), (b) PV array voltage and current (C-HIL experiment), (c) Power grid voltage and current (simulation), (d) Power grid voltage and current (C-HIL experiment), and (e) Power grid active power and PV array power.

B. Incremental Conductance Method

As demonstrated in Figures 6(a) and 6(b), the same as the P&O algorithm, the incremental conductance method starts at t = 0.15 s, and the maximum voltage and current of the PV array occur at t = 0.2 s. The achieved maximum voltage and current of the PV array using the incremental conductance method are 421.3 V and 5.11 A, respectively. When the solar irradiance is minimum, the voltage and current of the PV array are 406 V and 3.49 A, respectively. When atmospheric conditions vary rapidly, the incremental conductance method achieves the maximum power point quickly and efficiently. The C-HIL experiment results show that the maximum voltage and current of the PV array using the incremental conductance method are 421.1 V and 5.1 A, respectively. Consequently, the C-HIL experiment results show the performance of the incremental conductance method in real-world applications.

According to Figures 6(c) and 6(d), since the inverter, the DC–link capacitor, and the output filter losses are neglected, no voltage drop across the power grid occurs, which leads to maintaining the power grid voltage at 169.70 V. It should be noted that the minimum and maximum power grid current using the incremental conductance method are 25.15 A and 16.22 A, respectively. Additionally, the C-HIL experiment results show that the power grid current changes within the range of 16.56 A and 24.57 A, which is in close agreement with simulation results.

As shown in Figure 6(e), the average PV array power and average power grid active power using the incremental conductance method are 1908.40 W and 1854.20 W, respectively. The minimum PV array power and power grid active power occur at t = 1.5 s, where the PV array power is 1455.40 W and the power grid active power is 1363.1 W. According to Figure

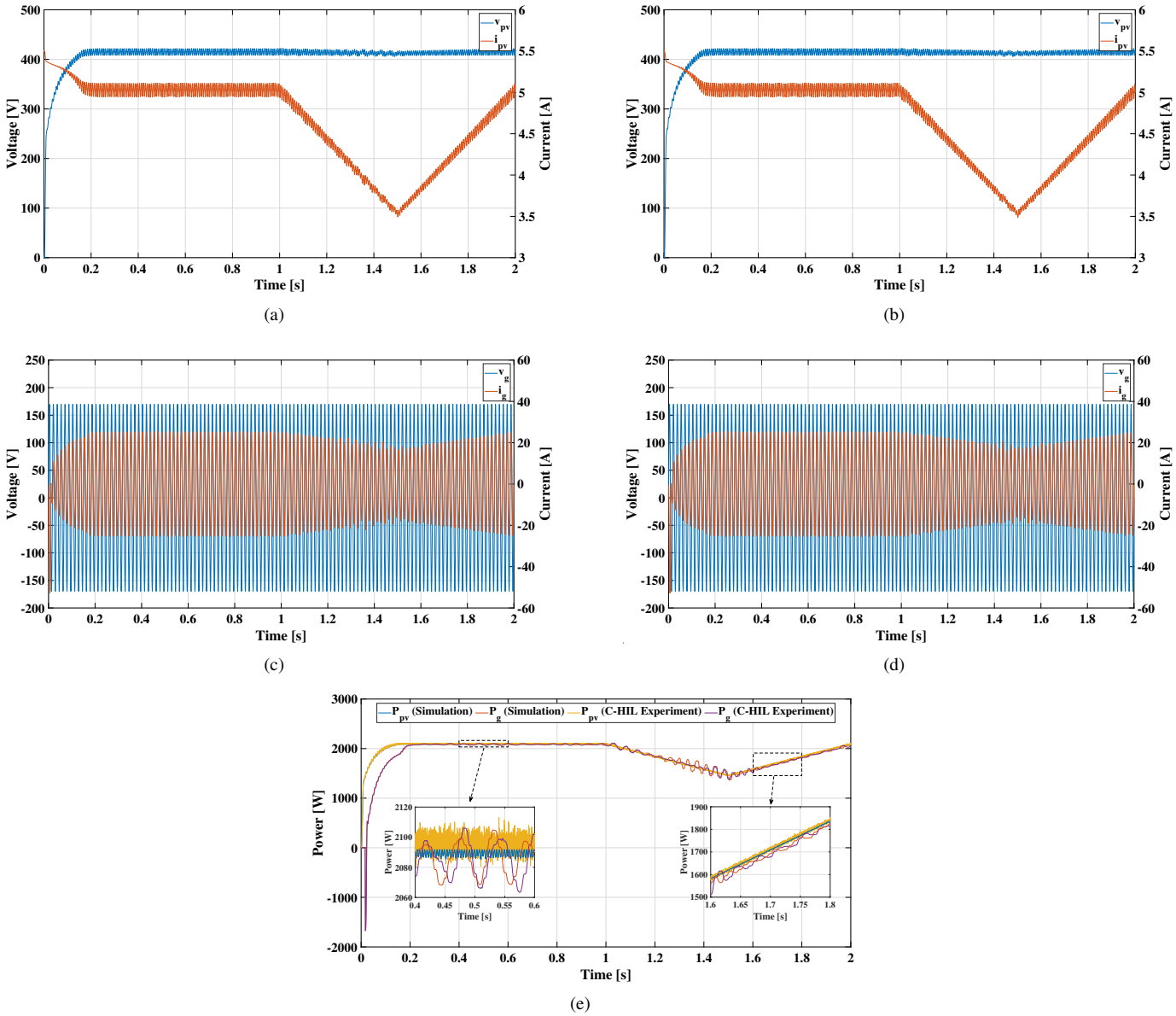

Figure 6. Results for the incremental conductance method, (a) PV array voltage and current (simulation), (b) PV array voltage and current (C-HIL experiment), (c) Power grid voltage and current (simulation), (d) Power grid voltage and current (C-HIL experiment), and (e) Power grid active power and PV array power.

6(e), between t = 0.4 s and t = 0.6 s, the C-HIL experiment results show that the average PV array power and average power grid active power using the incremental conductance method are 1913.20 W and 1854.34 W, respectively. Hence, the C-HIL experiment results verify the applicability of the presented control scheme.

C. Discussions

Figure 7 shows the C-HIL experiment results for the performance comparison between the P&O algorithm and incremental conductance method. As shown in this figure, the incremental conductance method has a higher efficiency in the steady-state. Indeed, both the PV array power and current using the incremental conductance method are higher than the P&O algorithm. In addition, this method reaches the maximum power point faster with reasonable dynamics compared to the P&O algorithm.

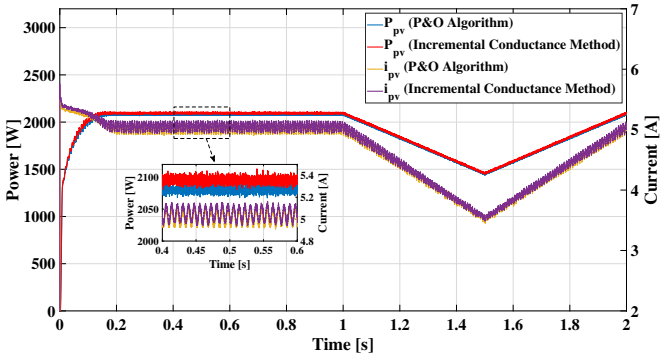

Figure 7. The C-HIL experiment results for performance comparison between the P&O algorithm and incremental conductance method.

According to Figure 7, between t = 0.4 s and t = 0.6 s, the C-HIL experiment results for the P&O algorithm show that

the PV array power and current deviate within the range of 2070 W and 2092 W, and 4.92 A and 5.10 A, respectively. During the same time interval, the C-HIL experiment results for the incremental conductance method demonstrate that the PV array power and current deviate within the range of 2080 W and 2113 W, and 4.95 A and 5.13 A, respectively.

IV. Conclusions

This paper presents a control scheme for a single-phase single-stage transformerless grid-connected Photovoltaic (PV) inverter. The presented control scheme consists of two control loops, namely as DC–link voltage and current control loops along with grid synchronization based on Phase Locked Loop (PLL). The Perturb and Observe (P&O) algorithm and incremental conductance method are utilized to extract the maximum power point from the PV array. To evaluate the performance of the presented control scheme, the Control-Hardware-in-the-Loop (C-HIL) testing using a LAUNCHXL-F28379D development kit is performed. The simulation and experimental results verify the applicability and effectiveness of the presented control scheme.

References

[1] F. Mohammadi, G.-A. Nazri, M. Saif, "A Bidirectional Power Charging Control Strategy for Plug-in Hybrid Electric Vehicles," *Sustainability*, Vol. 11(16), Aug. 2019.

[2] R. Zahedi, P. Ranjbaran, G. B. Gharehpetian, F. Mohammadi, R. Ahmadiahangar, "Cleaning of Floating Photovoltaic Systems: A Critical Review on Approaches from Technical and Economic Perspectives," *Energies*, Vol. 14(7), Apr. 2021.

[3] F. Mohammadi, M. Neagoe, "Emerging Issues and Challenges with the Integration of Solar Power Plants into Power Systems," *Solar Energy Conversion in Communities*, Springer Proceedings in Energy. Cham, Switzerland, Springer, Sep. 2020.

[4] IEEE Std 1547-2018, "IEEE Standard for Interconnection and Interoperability of Distributed Energy Resources with Associated Electric Power Systems Interfaces," Apr. 2018.

[5] IEC 61727:2002, "Photovoltaic (PV) Systems - Characteristics of the Utility Interface," Dec. 2004.

[6] A. Elmelegi, M. Aly, E. M. Ahmed, A. G. Alharbi, "A Simplified Phase-Shift PWM-Based Feedforward Distributed MPPT Method for Grid-Connected Cascaded PV Inverters," *Solar Energy*, Vol. 187, Jul. 2019.

[7] A. Amir, A. Amir, J. Selvaraj, N. A. Rahim, "Study of the MPP Tracking Algorithms: Focusing the Numerical Method Techniques," *Renewable and Sustainable Energy Reviews*, Vol. 62, Sep. 2016.

[8] D. Pilakkat, S. Kanthalakshmi, "An Improved P&O Algorithm Integrated with Artificial Bee Colony for Photovoltaic Systems Under Partial Shading Conditions," *Solar Energy*, Vol. 178, Jan. 2019.

[9] L. Shang, H. Guo, W. Zhu, "An Improved MPPT Control Strategy Based on Incremental Conductance Algorithm," *Protection and Control of Modern Power Systems*, Vol. 5, Jun. 2020.

[10] D. Kolantla, S. Mikkili, S. R. Pendem, A. A. Desai, "Critical Review on Various Inverter Topologies for PV System Architectures," *IET Renewable Power Generation*, Vol. 14(17), Dec. 2020.

[11] F. Mohammadi, B. Mohammadi-Ivatloo, G.-B. Gharehpetian, M. Hasan Ali, W. Wei, O. Erdinç, M. Shirkhani, "Robust Control Strategies for Microgrids: A Review," *IEEE System Journal*, Jun. 2021.

[12] E. Villanueva, P. Correa, J. Rodriguez, M. Pacas, "Control of a Single-Phase Cascaded H-Bridge Multilevel Inverter for Grid-Connected Photovoltaic Systems," *IEEE Transactions on Industrial Electronics*, Vol. 56(11), Nov. 2009.

[13] H. Patel, V. Agarwal, "A Single-Stage Single-Phase Transformer-Less Doubly Grounded Grid-Connected PV Interface," *IEEE Transactions on Energy Conversion*, Vol. 24(1), Mar. 2009.

[14] D. Zammit, C. Spiteri Staines, M. Apap, "Comparison Between PI and PR Current Controllers in Grid Connected PV Inverters," *International Journal of Electrical and Computer Engineering*, Vol. 8(2), Jan. 2014.

[15] S. A. Lakshmanan, A. Jain, B. S. Rajpourhit, "A Novel Current Controlled Technique with Feed Forward DC Voltage Regulator for Grid Connected Solar PV System," *2014 Eighteenth National Power Systems Conference*, Dec. 2014.

[16] H. K. Yada, B. A. Kumar, V. P. Muddineni, "A Second Order-Second Order Generalized Integrator for Three-Phase Single-Stage Multifunctional Grid-Connected SPV System," *2020 International Conference on Smart Technologies in Computing, Electrical and Electronics*, Oct. 2020.

[17] M. Ciobotaru, R. Teodorescu, F. Blaabjerg, "Control of Single-Stage Single-Phase PV Inverter," *2005 European Conference on Power Electronics and Applications*, Sep. 2005.

[18] P. Rodriguez, J. Pou, J. Bergas, J. I. Candela, R. P. Burgos, D. Boroyevich, "Decoupled Double Synchronous Reference Frame PLL for Power Converters Control," *IEEE Transactions on Power Electronics*, Vol. 22(2), Mar. 2007.